Measurement accuracy of foot conformation parameters on low-field magnetic resonance images in horses

David M. Bolt [a],*, Mary E. Carrier [a], Kate S. Sheridan [a], Gabriel Manso-Diaz [b], Dagmar Berner [a]

[a] *Equine Referral Hospital, Department of Clinical Science and Services, Royal Veterinary College, Hatfield, United Kingdom*
[b] *Hospital Clinico Veterinario Complutense, Universidad Complutense de Madrid, Madrid, Spain*

ABSTRACT

Foot imbalance and malalignment of the digits are common in horses. Angle and distance measurements performed on bones, joints and hoof wall on radiographs provide essential guidance for precise corrective trimming and shoeing. This study aimed to investigate, if selected standing low-field magnetic resonance (MR) images can be used to accurately measure dorsopalmar and lateromedial foot conformation parameters in comparison to the radiographic gold standard. Images of 100 horses referred for standing low-field MR examination were selected. Foot conformation angles and distances were measured and compared between radiographs and MR images. Measurements from most imaging sources were significantly different from each other. Moderate to high correlation of foot conformation angles between radiographs and MR images in the lateromedial and dorsopalmar planes was found, with exception of the proximal interphalangeal joint angle, where there was only moderate agreement between radiographs and the 5-plane MR pilot (0.47, *P* < .001) and between radiographs and the 3-plane MR pilot (0.4, *P* < .001), respectively. Measurement of foot conformation parameters from low-field MR images should be used with caution in clinical practice and acquisition of current foot radiographs immediately before or after MR examination should be considered to facilitate precise trimming and shoeing.

© 2022 The Authors. Published by Elsevier Inc.
This is an open access article under the CC BY license (http://creativecommons.org/licenses/by/4.0/)

1. Introduction

Corrective farriery, by itself or in combination with other surgical or medical treatments, is one of the most used modalities to prevent or manage lameness in horses [1, 2].

Although foot imbalance and variability in conformation parameters have been associated with certain bone or soft tissue lesions within the hoof capsule [3], identification of a defined foot conformation as the single causative factor of lameness is usually not possible. This is mainly because changes in foot conformation can result in lameness, but foot conformation itself can also change as a consequence of lameness [4]. Foot imbalance and malalignment of the digits are very common and have been found to be present in 72.8% of horses presenting with forelimb lameness [5]. The distal forelimb of the horse sustains the highest stress during movement and both the distal and proximal interphalangeal joints undergo a considerable amount of impact during movement [6]. Due

to its overall higher mobility, the distal interphalangeal joint has been shown to be more affected by variations in foot placement and its conformational parameters are also more directly affected by trimming and shoeing changes [6].

Distal limb conformation in horses is assessed from lateral (hoof pastern axis, dorsopalmar foot conformation), dorsal (lateromedial foot conformation), palmar, solar and rotational perspectives. Angles, as well as distance measurements (length and width) on bones, joints and hoof wall on radiographs can provide useful guidance for corrective trimming and balancing of feet and for application of therapeutic shoes [2, 7]. A high degree of precision in this process is considered important, as clinical decisions are often made based on a difference of only a few degrees angulation [1]. On lateromedial radiographs, these measurements include, but are not limited to, the dorsal hoof wall angle, the solar angle and the length of the weight-bearing surface of the hoof dorsal and palmar to the intersection with a vertical line extending from the center of rotation of the distal interphalangeal joint [7]. Dorsopalmar radiographs are assessed for lateral and medial hoof wall angles, hoof wall lengths and widths, as well as the angles of distal and proximal interphalangeal joints among other parameters [7].

* Corresponding author at: David M. Bolt, Dr. med. vet., MRCVS, Equine Referral Hospital, Royal Veterinary College, Hawkshead Lane, Hatfield, Hertfordshire, AL7 9TA, UK.

E-mail address: dbolt@rvc.ac.uk (D.M. Bolt).

Standing low-field magnetic resonance (MR) examination has become widely available in equine orthopedics and represents an essential imaging modality for identification of soft tissue lesions and certain bone lesions within the hoof capsule [8, 9]. Many conditions identified with MR imaging result in recommendations for therapeutic trimming and shoeing along with other treatments. In clinical practice, measurement of angles and distances for this purpose is most often performed on radiographs. These are not always obtained at the time of MR examination and previously measured parameters may therefore no longer reflect the current foot conformation. On the other hand, obtaining new and current foot radiographs results in additional cost to the client and in radiation exposure of staff. Radiographs are therefore not always repeated at the time of the MR scan.

The aim of the present study was to investigate if pilot images and T1-weighted gradient echo (T1W GRE) images in frontal and sagittal scans from standing low-field MR examination are suitable to adequately measure selected dorsopalmar and lateromedial foot conformation parameters in horses in comparison to the radiographic gold standard. We hypothesized that foot conformation parameters obtained from MR images are not significantly different from those obtained from radiographs obtained at the time of MR examination.

2. Materials and Methods

The records of horses referred to RVC Equine for standing low-field MR examination of the forefeet between May 2017 and February 2019 were reviewed. Animals were considered for inclusion in the study, if weight-bearing lateromedial and straight dorsopalmar digital radiographs (Veterinary Xrays Powerlight, Veterinary Xrays, Princes Risborough, United Kingdom; exposure settings: 60-64kV, 3.10-3.36mAs) along with sagittal and frontal standing low-field uncorrected pilot and T1-weighted (T1W) gradient recalled echo (GRE) MR images (EQ2, Hallmarq Veterinary Imaging, Guildford, United Kingdom) had been obtained. Image quality and suitability for inclusion in the study was assessed by a Diplomate ECVDI (DaBe).

An online sample size calculator (ClinCalc.com) was used to perform a power analysis based on pilot data (10 cases). The results varied highly between different parameters that were tested (12-120). One-hundred horses were therefore randomly chosen out of all patients meeting inclusion criteria and images of the right fore foot were analyzed for each case.

Radiographs and MR images were uploaded into a free DICOM viewing software (horosproject.org, sponsored by Nimble Co LLC Purview, 2020). No markers allowing for correction of magnification were used in these clinical cases due to the retrospective nature of the study. A single observer (KSS) measured selected dorsopalmar foot conformation parameters, and another single observer (MEC) measured selected parameters for lateromedial foot conformation. All parameters were measured three times and the mean value was used for analysis.

2.1. Dorsopalmar Foot Conformation Parameters

The lateromedial radiographic view of the foot, the optimally piloted sagittal image from the 3-plane MR study pilot and the central (most axial) sagittal T1W GRE MR image (slice thickness 2mm, echo time 7ms, repetition time 24 ms, flip angle 45 degrees) were assessed. The latter MR sequence was added due to the observed reduced visibility of the outline of the hoof capsule on MR pilot images. The dynamic angle tool was used to measure the following angles in each image: (1) SSH: Angle between the concave solar surface of the distal phalanx and horizontal [4]. (2)

HWH: Angle between the dorsal hoof wall and horizontal. To obtain this angle on radiographs, a line was drawn parallel to the dorsal hoof wall. For measurements on MR images, the most proximal aspect of the hoof wall just distally to the outline of the periople (which is fully visible on MR images) was used as a reference point and a line paralleling the visible dermis was extended distad. (3) DSH: Angle between the dorsal surface of the distal phalanx and horizontal (Fig. 1). The total weight-bearing surface of the hoof (TWBS), as well as the dorsal (DWBS) and palmar (PWBS) weight-bearing surfaces, separated by a vertical line extending distad from the center of rotation of the distal interphalangeal joint, were individually measured with the ruler tool. The center of rotation of the distal interphalangeal joint was determined as the center of a circle drawn with the circle tool that follows the distal margin of the trochlea of the middle phalanx (Fig. 2).

2.2. Lateromedial Foot Conformation Parameters

The dorsopalmar radiographic view of the phalanges and the frontal 3-plane and 5-plane MR pilot images were analyzed. The single frontal image of the 3-plane pilot was centered on the palmar aspect of the distal part of the middle phalanx at lateromedial mid-distance. Two frontal images were acquired for the 5-plane MR pilot. These were re-piloted to be parallel to the palmar border of the navicular bone. The image best outlining the distal aspect of the middle or proximal phalanx, respectively, was selected for analysis. The dynamic angle tool was used to measure the following angles: (1) DistP2: Angle between the distal articular surface of the middle phalanx and horizontal (coffin joint angle) and (2) DistP1: Angle between the distal articular surface of the proximal phalanx and horizontal (pastern joint angle, Fig. 3).

3. Data Analysis

The mean value for each measurement was entered on a Microsoft Excel data sheet. A free programming language software (R project for statistical computing, Version 4.0.3, r-project.org) was used for data analysis. Descriptive statistics for all measured parameters were obtained and data were tested for normal distribution using the Shapiro-Wilk test. Measurements between different imaging modalities and settings were compared using Kendall's rank correlation tau and Wilcoxon paired signed-rank tests. Bland-Altman plots were created for the combinations of imaging modalities. Intraobserver reliability over the three measurements of each parameter from each imaging source was assessed by calculating Spearman's rho. A P value of $< .05$ was considered significant.

4. Results

Most data were non-normally distributed and non-parametric tests were therefore utilized. The descriptive statistics of parameters for dorsopalmar and lateromedial foot conformation with different imaging techniques are summarized in Table 1 and Table 2, respectively (Figs. 4–6). There was a low to high positive correlation between angles and lengths measured from all image sources for both dorsopalmar and lateromedial parameters. However, comparison with the Wilcoxon paired signed rank test identified significant differences between most image sources.

4.1. Dorsopalmar Foot Conformation Parameters

The rank correlation between all measured angles (SSH, HWH and DSH) from different image sources was highly positive and ranged from 0.73 to 0.86 ($P < .001$, Table 3). However, angle measurements were significantly different between images sources
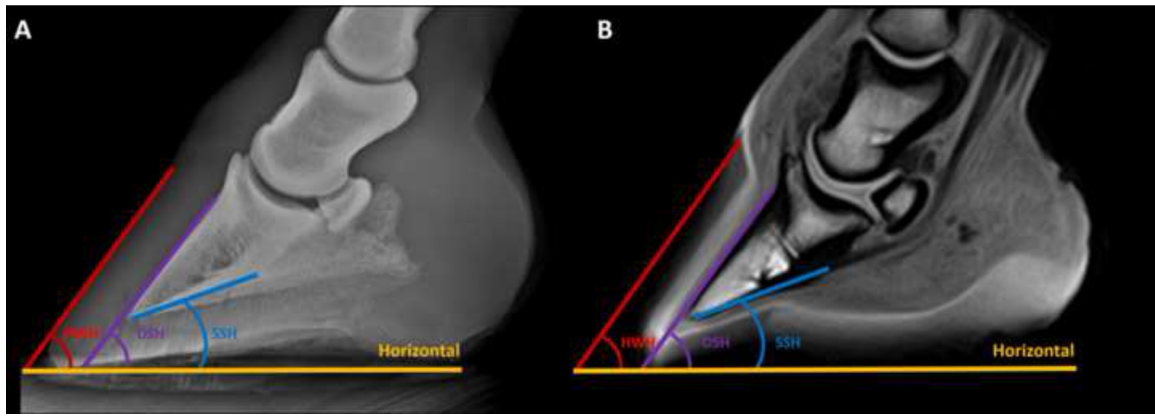
Fig. 1. Dorsopalmar foot conformation angles measured on lateromedial radiograph (A) and the sagittal T1W GRE MR image (B). SSH = Angle between the concave solar surface of the distal phalanx and horizontal, HWH = Angle between the dorsal hoof wall and horizontal, DSH = Angle between the dorsal surface of the distal phalanx and horizontal.
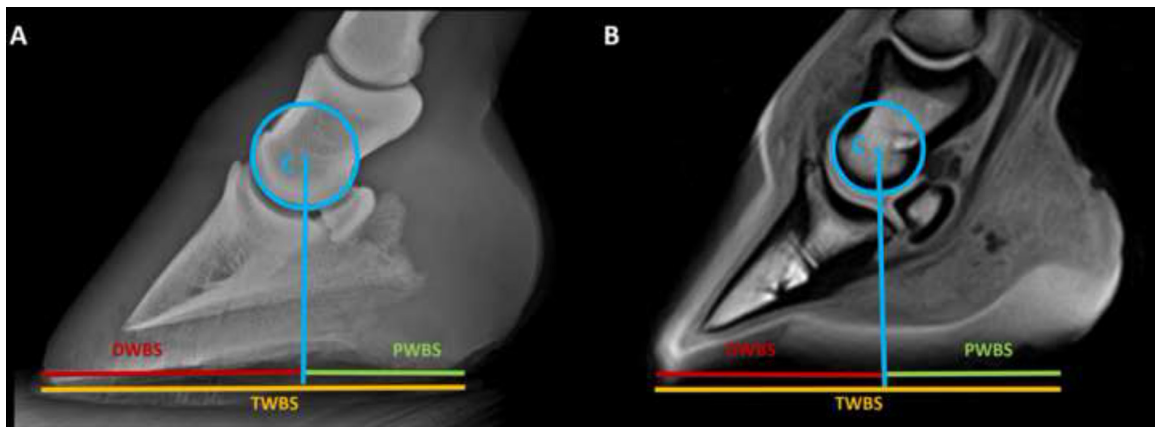

Fig. 2. Dorsopalmar weight-bearing solar surface measurements on lateromedial radiograph (A) and sagittal T1W GRE MR image (B). TWBS = total weight-bearing surface of the hoof, DWBS = dorsal weight-bearing surface, PWBS = palmar weight-bearing surface, C = centre of rotation of the distal interphalangeal joint.
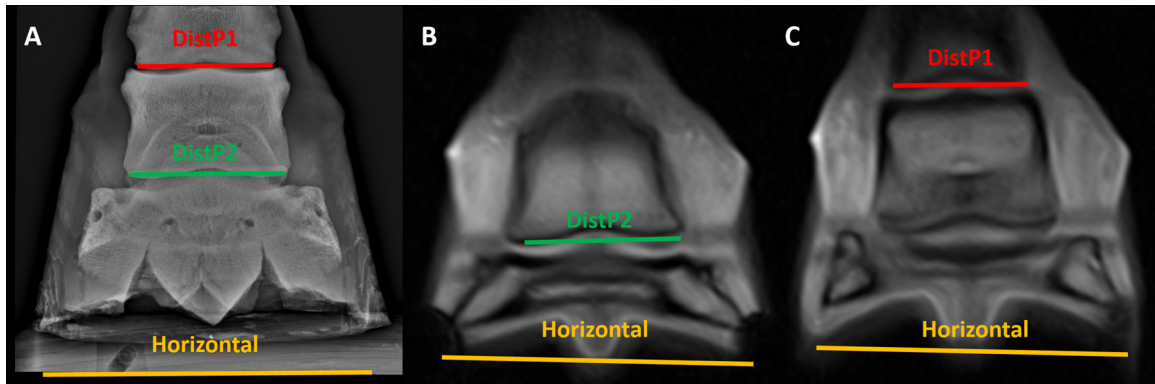

Fig. 3. Lateromedial foot conformation angles measured on dorsopalmar radiograph (A), dorsal frontal image (B) and palmar frontal image (C) from 5-plane MR pilot. DistP2 = distal interphalangeal joint angle, DistP1 = proximal interphalangeal joint angle.

with exception of the comparison between HWH angles from radiographs and sagittal MRI pilot images: SSH and DSH were consistently measured lower on radiographs than on both MR sources, whereas SSH, HWH and DSH was measured higher on T1W GRE MR images than on the 3-plane MR study pilot images (Fig. 4). The correlation of the measured lengths of the weight-bearing surface of the foot between image sources was found to range from low (0.32) to high (0.61, $P < .001$, Table 4). Subjectively, the outline of the hoof capsule was better visualized on T1W GRE MR images than on sagittal MRI pilot images. All length measurements were significantly different from each other between the three image sources with exception of the comparison of PWBS measurements

from radiographs and sagittal MRI pilot images. DWBS and TWBS consistently measured higher on radiographs than on both MR image sources. There was no significant difference in PWBS measurements between the 3-plane MR study pilot images and radiographs and in TWBS measurements between T1W GRE MR images and the 3-plane MR study pilot images (Fig. 5).

4.2. Lateromedial Foot Conformation Parameters

The rank correlation for the DistP2 angle between the 3-plane pilot MR image, the 5-plane pilot MR image and the dorsopalmar radiographic view ranged from 0.39 to 0.6. The highest cor-

Table 1
Descriptive data of dorsopalmar foot conformation measurements.

Parameter	Minimum	Q25	Median	Mean	SD	Variance	Q75	Maximum	Range	Normality
SSH Pil	7.11	12.49	14.47	15.27	4.49	20.13	18.18	25.60	18.49	No
SSH T1	6.84	11.54	14.62	14.91	4.44	19.73	17.67	25.77	18.93	No
SSH Rad	6.64	11.28	13.74	14.44	4.45	19.76	17.49	25.21	18.57	No
HWH Pil	40.57	46.59	49.18	48.90	3.64	13.26	51.05	58.07	17.50	Yes
HWH T1	41.57	47.61	49.35	49.47	3.57	12.75	51.81	59.55	17.98	Yes
HWH Rad	40.31	46.85	49.02	48.89	3.44	11.82	51.03	57.73	17.42	Yes
DSH Pil	39.99	46.54	48.29	48.59	3.65	13.35	50.75	60.30	20.31	Yes
DSH T1	42.26	47.16	49.12	49.22	3.45	11.87	51.39	60.49	18.23	No
DSH Rad	41.21	45.93	47.76	48.10	3.38	11.43	49.92	58.15	16.94	No
DWBS Pil	5.01	6.32	6.66	6.66	0.53	0.28	6.99	7.88	2.87	Yes
DWBS T1	5.18	6.51	6.87	6.82	0.49	0.24	7.14	8.21	3.03	Yes
DWBS Rad	7.53	9.04	9.69	9.72	0.96	0.93	10.31	13.82	6.29	No
PWBS Pil	4.11	5.36	5.79	5.73	0.59	0.34	6.15	7.29	3.18	Yes
PWBS T1	4.31	5.26	5.72	5.67	0.54	0.29	5.97	7.16	2.85	Yes
PWBS Rad	4.31	5.39	5.83	5.90	0.83	0.68	6.29	8.48	4.17	No
TWBS Pil	10.53	11.90	12.44	12.39	0.70	0.50	12.81	14.14	3.61	Yes
TWBS T1	10.76	12.06	12.52	12.49	0.65	0.42	12.85	14.01	3.25	Yes
TWBS Rad	13.10	14.75	15.51	15.62	1.42	2.01	16.32	22.21	9.11	No

DSH, angle between the dorsal surface of the distal phalanx and horizontal (degrees); DWBS, dorsal weight-bearing surface (cm); HWH, angle between the dorsal hoof wall and horizontal (degrees); Maximum, maximal value; Minimum, minimal value; Median, median value; Mean, mean value; Normality, normally distributed (yes/no) ; PWBS, palmar weight-bearing surface (cm; Pil, sagittal images from 3-plane MRI pilotsRad, lateromedial radiographic view; Q25, first quartile; Range, range of values; SD, standard deviation; Variance, variance; SSH, angle between the solar surface of the distal phalanx and horizontal (degrees); T1, images from sagittal T1-weighted MR sequence); TWBS, total weight-bearing surface (cm).

Table 2
Descriptive data of lateromedial foot conformation measurements.

Parameter	Minimum	Q25	Median	Mean	SD	Variance	Q75	Maximum	Range	Normality
DistP2 M3P	0.15	0.57	0.81	0.99	0.64	0.41	1.25	3.49	3.34	No
DistP2 M5P	0.24	0.57	0.83	0.95	0.55	0.30	1.14	2.71	2.47	No
DistP2 Rad	0.07	0.52	0.98	1.22	0.87	0.76	1.78	3.82	3.75	No
DistP1 M3P	0.20	0.77	1.29	1.38	0.77	0.59	1.85	3.56	3.36	No
DistP1 M5P	0.23	0.89	1.37	1.48	0.79	0.62	1.96	3.88	3.65	No
DistP1 Rad	0.14	0.74	1.26	1.53	1.01	1.02	2.17	5.52	5.38	No

DistP1, angle between the articular surface of the proximal interphalangeal joint and horizontal (pastern joint angle, degrees); DistP2, Angle between the articular surface of the distal interphalangeal joint and horizontal (coffin joint angle, degrees); M3P, sagittal images from 3-plane MRI pilots; M5P, sagittal images from 5-plane MRI pilots; Minimum, minimal value; Median, median value; Mean, mean value; Maximum, maximal value; Q25, first quartile; Range, range of values, Normality, normally distributed (yes/no); Rad, dorsopalmar radiographic view; SD, standard deviation; Variance, variance.

relation (0.6, $P < .001$) was found between measurements of the DistP2 angle from 3-plane pilot MR images and from 5-plane pilot MR images. There was also no significant difference between measurements of this angle between the two MR pilot images sources ($V = 2450.5$, $P = .93$). There was a significant difference between DistP2 angle measurements obtained from radiographs and both MR pilot images (Table 5, Fig. 6).

The rank correlation for the DistP1 angle between the 3-plane pilot MR image, the 5-plane pilot MR image and the dorsopalmar radiographic view ranged from 0.4 to 0.59 ($P < .001$). There was no significant difference for this angle between radiographs and either MRI pilot or between the two MRI pilots (Table 5, Fig. 6).

4.3. Intraobserver reliability

Intraobserver reliability for repeated measurements of each foot conformation parameter was high with Spearman's rho ranging from 0.762 ($P < .001$, CI 0.66-0.84) for PWBSPil to 0.993 ($P < .001$, CI 0.99-1.0) for DWBSRad.

5. Discussion

The present study has identified a low to high degree of positive correlation between foot conformation angles and lengths measured from radiographs and MR images in both the lateromedial and dorsopalmar planes. However, with few exceptions, the measured dorsopalmar foot conformation parameters between the different image sources were found to be significantly different from each other. With regards to lateromedial conformation, there was a significant difference for the distal interphalangeal joint angle DistP2 between radiographs and the two MR image sources, but there were no significant differences between all imaging sources for the proximal interphalangeal joint angle DistP1. Overall, the hypothesis of the study was therefore rejected.

Exact measurement of foot conformation angles and distances is considered useful and supportive for correct trimming and appropriate choice of shoeing in horses [1, 2, 5, 7]. A significant difference between image sources for most measured parameters was identified with the robust Wilcoxon signed-rank test in our study. Similar to findings in the study from Arble et al. (2009), this could indicate a truly inferior suitability of MR images for this purpose in comparison to the radiographic gold standard [10]. Variable inter- and intraobserver reliability is not unusual in studies evaluating diagnostic imaging studies of orthopedic conditions [11, 12], although a previous multi-observer study assessing selected equine hoof wall and sole measurements on radiographs and MR images has identified excellent inter- and intraobserver reliability [13]. Measurements for both dorsopalmar and lateromedial conformation parameters in the present study were performed by single two observers, respectively. The intraobserver reliability in our study was high, with a Spearman rho between the three measurements of each parameter ranging from 0.762 to 0.993. However, intraobserver reliability is often higher than interobserver reliabil-
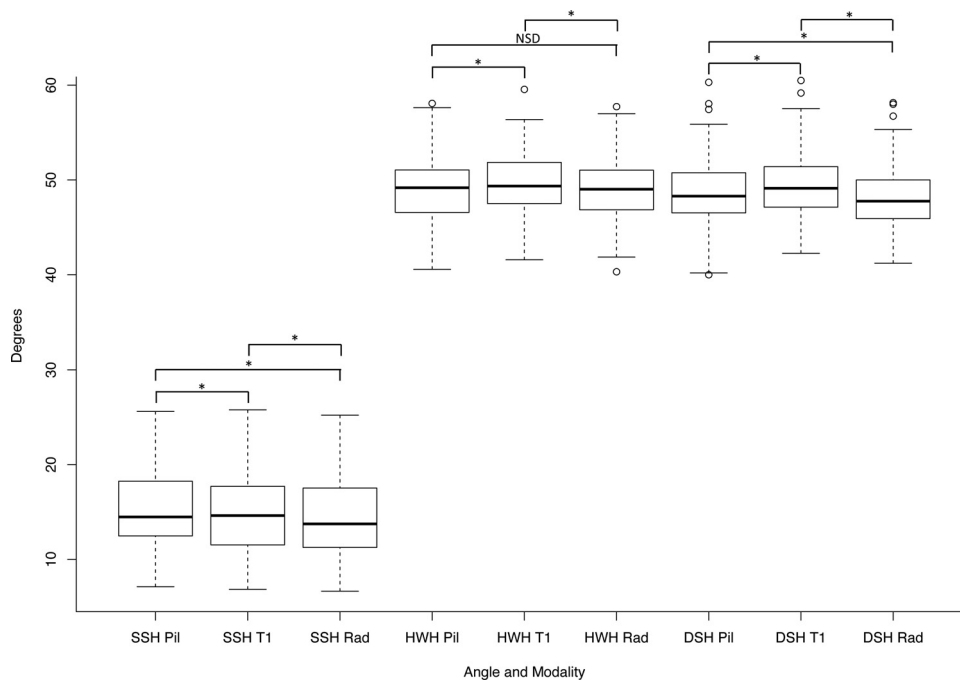
Fig. 4. Box-and-whisker plots of dorsopalmar foot conformation angles. Bold horizontal bar = median, box = interquartile range, bottom whisker = Minimum (first quartile -1.5x interquartile range), top whisker = Maximum (third quartile + 1.5 x interquartile range), circles = outliers. SSH = SSH angle, HWH = HWH angle, DSH = SDH angle, Pil = sagittal images from 3-plane MR pilot, T1 = images from sagittal T1-weighted MR sequence, Rad = lateromedial radiographic view. Asterisk indicates significant difference. NSD = No significant difference.
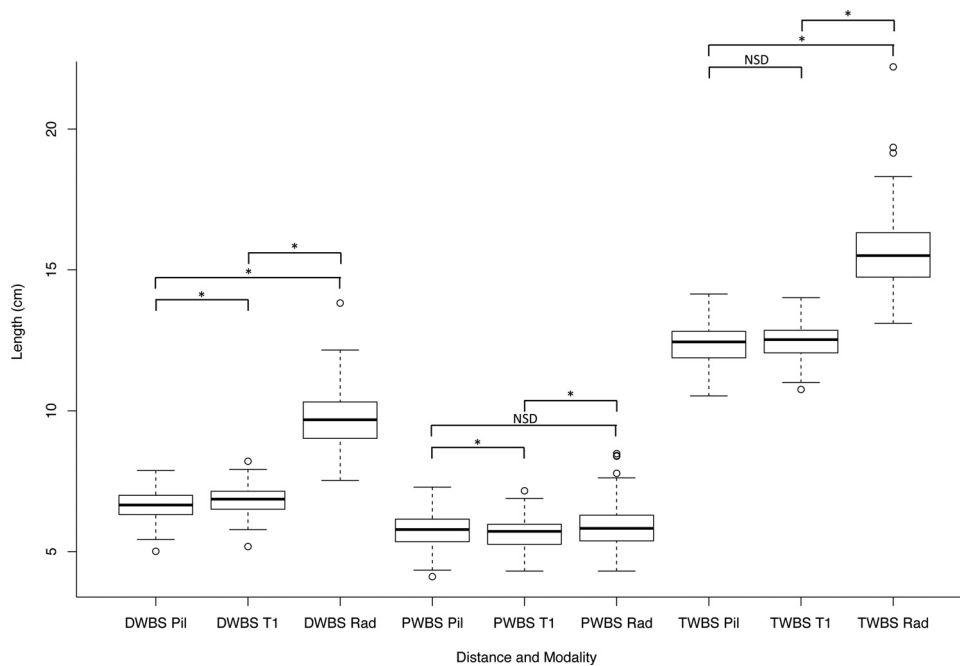
Fig. 5. Box-and-whisker plots of dorsopalmar foot conformation lengths. Bold horizontal bar = median, box = interquartile range, bottom whisker = Minimum (first quartile -1.5x interquartile range), top whisker = Maximum (third quartile + 1.5 x interquartile range), circles = outliers. DWBS = dorsal weight-bearing surface, PWBS = palmar weight-bearing surface, TWBS = total weight-bearing surface, Pil = sagittal images from 3-plane MR pilots, T1 = images from sagittal T1-weighted MR sequence, Rad = lateromedial radiographic view. Asterisk indicates significant difference. NSD = No significant difference.

ity in the analysis of diagnostic imaging studies [11, 12]. The use of more observers could therefore potentially have produced different results.

Inaccurate measurement of conformation angles and distances could also have been caused by the less distinctly visible outline of the hoof capsule on MR images in comparison to radiographs. The hoof wall, particularly the stratum externum and the stratum

medium, has a relatively low water content. Consequently, the low number of hydrogen ions in these tissues results in less signal and poorer image quality in some MR sequences [13]. As this was merely a problem for the measurement of dorsopalmar conformation parameters, we have decided to additionally include analysis of sagittal T1W GRE MR images for this part of the study. Subjectively, we felt that the outline of the hoof capsule was better
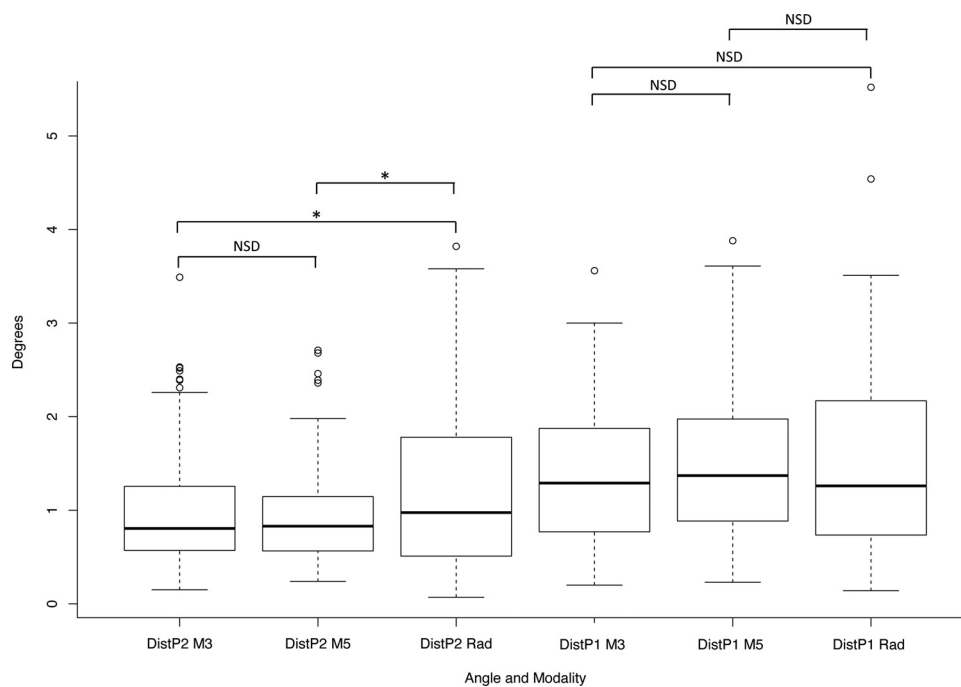
Fig. 6. Box-and-whisker plots of lateromedial foot conformation angles. Bold horizontal bar = median, box = interquartile range, bottom whisker = Minimum (first quartile - 1.5x interquartile range), top whisker = Maximum (third quartile + 1.5 x interquartile range), circles = outliers, DistP2 = distal interphalangeal joint angle, DistP1 = proximal interphalangeal joint angle, M3 = sagittal images from 3-plane MR pilot, M5 = sagittal images from 5-plane MR pilot, Rad = dorsopalmar radiographic view. Asterisk indicates significant difference. NSD = No significant difference.

visible on images from this MR sequence in comparison to images from the MR pilot sequence. However, the values for HWH obtained from MR images tended to be higher than those obtained from radiographs: The difference was significant between measurements from T1W GRE MR images and those from radiographs. This observation could potentially be explained by the technique used for measuring HWH on MR images, with the periople providing the only reliable directly visible landmark indicating the contour of the dorsal hoof wall. Also, DWBS and TWBS measurements in sagittal MR images were significantly shorter in comparison to those obtained from lateromedial radiographs, which was attributed to poor visibility of the solar surface of the hoof capsule. In their cadaver model study, Grundmann et al. (2015) have improved the visibility of the hoof capsule outline by coating it with lard prior to high-field MR image acquisition in order to saturate the superficial keratin with more moisture. The authors felt that this allowed for precise and consistent measurements in the hoof wall and sole [13]. In the same study, the authors also applied a thin layer of barium contrast paste to the sole to facilitate more exact and consistent measurement of foot conformation parameters from digital radiographs [13]. Due to its retrospective nature, no such measures to improve visibility of the hoof capsule outline with either imaging modality were undertaken in our study. For the same reason, we have also not used markers that would have allowed for correction of magnification on radiographs.

The concave solar angle of the distal phalanx (SSH) is not routinely used as a foot conformation parameter: The contour of the solar margin visible on a radiograph represents the summation of superimposing regions of the distal phalanx. This is not adequately represented on a single slice of a 3D imaging modality, such as MR. On the other hand, the concave solar angle of the distal phalanx (SSH) can be measured on both lateromedial radiographic views and mid-sagittal MR images [4].

Different positioning of the limb during image acquisition with the respective modalities could have been another confounding factor. Image quality and foot conformation parameters can be con-

siderably altered by changes in positioning of the limb: Increasing degrees of abduction of the forelimb during acquisition of dorsopalmar foot radiographs in live horses have been shown to result in significant increase of the distal and proximal interphalangeal joint angles [14].

We have not observed this in our study: With positioning of the limb in the open magnet of the standing MR system, we would have expected both DistP2 and DistP1 to be higher on MR images than on radiographs. However, DistP2 angle was significantly higher on radiographs than on MR images. Also, DistP1 was measured higher than DistP2 in all imaging sources. Whereas the former observation could potentially be explained with a higher degree of abduction during acquisition of radiographs (despite all efforts made to position the limbs correctly), we have no conclusive explanation for the latter: Overall, the observed differences between imaging modalities were very small (1-2 degrees). These results should therefore be interpreted with caution, as it is possible that they do not indicate a true disparity. Retrospectively, measurement of an additional pedal bone angle [2] could potentially have provided more information about the effects of limb abduction. Also, a cadaver limb study by Tacchio et al. (2002) has demonstrated that rotation of the hoof also must be tightly controlled to allow for consistent measurement of dorsopalmar foot conformation angles [15]. Lastly, a unipodal stance (lifting the contralateral forelimb) during acquisition of foot radiographs has been shown to significantly alter multiple lateromedial and dorsopalmar foot conformation parameters [16]. It is therefore important to position the limb as straight as possible and to avoid abduction during acquisition of both radiographs and standing low-field MR images. In our experience, the width and height of the open low-field magnet makes this often difficult during MR examination, particularly in smaller horses where a certain amount of limb abduction cannot always be avoided.

In standing low-field MR studies in horses, only the first uncorrected pilot scan truly indicates the orientation of the foot in relation to the ground. However, in order to optimize image acqui-

Table 3
Correlation matrix and Wilcoxon paired signed-rank test results of angles measured for dorsopalmar foot conformation.

		SSH PIL	SSH T1	SSH RAD
SSH Pil	Kendalls' Tau		0.86	0.84
	P value		<0.001*	<0.001*
	V		3555.00	758.50
	P value		<0.001*	<0.001*
SSH T1	Kendalls' Tau	0.86		0.82
	P value	<0.001*		<0.001*
	V	3555.00		1462.00
	P value	<0.001*		<0.001*
SSH Rad	Kendalls' Tau	0.84	0.82	
	P value	<0.001*	<0.001*	
	V	758.50	1462.00	
	p-value	<0.001*	<0.001*	
		HWH Pil	HWH T1	HWH Rad
HWH Pil	Kendalls' Tau		0.81	0.73
	P value		<0.001*	<0.001*
	V		1159.00	2515.00
	P value		<0.001*	0.97
HWH T1	Kendalls' Tau	0.81		0.73
	P value	<0.001*		<0.001*
	V	1159.00		1311.00
	P value	<0.001*		<0.001*
HWH Rad	Kendalls' Tau	0.73	0.73	
	P value	<0.001*	<0.001*	
	V	2515.00	1311.00	
	P value	0.97	<0.001*	
		DSH Pil	DSH T1	DSH Rad
DSH Pil	Kendalls' Tau		0.81	0.79
	P value		<0.001*	0.000
	V		938.00	1296.50
	P value		<0.001*	<0.001*
DSH T1	Kendalls' Tau	0.81		0.82
	P value	<0.001*		<0.001*
	V	938.00		234.00
	P value	<0.001*		<0.001*
DSH Rad	Kendalls' Tau	0.79	0.82	
	P value	0.000	<0.001*	
	V	1296.50	234.00	
	P value	<0.001*	<0.001*	

DSH, angle between the dorsal surface of the distal phalanx and horizontal; HWH, angle between the dorsal hoof wall and horizontal; Kendall's tau, correlation coefficient with p-value; Pil, sagittal images from 3-plane MRI pilots; Rad, lateromedial radiographic view; SSH, angle between the solar surface of the distal phalanx and horizontal; T1, images from sagittal T1-weighted MR sequence; V, V-statistic Wilcoxon paired signed-rank test with p-value.

* indicates statistical significance.

Table 4
Correlation matrix and Wilcoxon paired signed-rank test results for length measurements of dorsopalmar foot conformation.

		DWBS Pil	DWBS T1	DWBS Rad
DWBS Pil	Kendalls' Tau		0.61	0.42
	P value		<0.001*	<0.001*
	V		1089.50	5050.00
	P value		<0.001*	<0.001*
DWBS T1	Kendalls' Tau	0.61		0.35
	P value	<0.001*		<0.001*
	V	1089.50		5050.00
	P value	<0.001*		<0.001*
DWBS Rad	Kendalls' Tau	0.42	0.35	
	P value	<0.001*	<0.001*	
	V	5050.00	5050.00	
	P value	<0.001*	<0.001*	
		PWBS Pil	PWBS T1	PWBS Rad
PWBS Pil	Kendalls' Tau		0.53	0.32
	P value		<0.001*	<0.001*
	V		3139.00	2872.00
	P value		0.03*	0.23
PWBS T1	Kendalls' Tau	0.53		0.35
	P value	<0.001*		<0.001*
	V	3139.00		3323.50
	P value	0.03*		0.006*
PWBS Rad	Kendalls' Tau	0.32	0.35	
	P value	<0.001*	<0.001*	
	V	2872.00	3323.50	
	P value	0.23	0.006*	
		TWBS Pil	TWBS T1	TWBS Rad
TWBS Pil	Kendalls' Tau		0.52	0.46
	P value		<0.001*	<0.001*
	V		4923.00	5050.00
	P value		0.05	<0.001*
TWBS T1	Kendalls' Tau	0.52		0.47
	P value	<0.001*		<0.001*
	V	4923.00		5050
	P value	0.05		<0.001*
TWBS Rad	Kendalls' Tau	0.46	0.47	
	P value	<0.001*	<0.001*	
	V	5050.00	5050	
	P value	<0.001*	<0.001*	

DWBS, dorsal weight-bearing surface; Kendall's tau, correlation coefficient with p-value; PWBS, palmar weight-bearing surface; Pil, sagittal images from 3-plane MRI pilots; Rad, lateromedial radiographic view; TWBS, total weight-bearing surface; T1, images from sagittal T1-weighted MR sequence; V, V-statistic Wilcoxon paired signed-rank test with P value.

* indicates statistical significance.

sition and visualization of structures, one or more follow-up pilot scans are often acquired to plan the subsequent diagnostic MR sequences of the study [17]. This step results in a rotation of planes and subsequently acquired images therefore no longer indicate the true orientation of the foot in relation to the ground. This could also explain the difference between some measured parameters from radiographs and from some of the MR images in the present study. Using the first, uncorrected 3-plane MR pilot scan only for analysis would avoid this problem, but the poorly visible outline of structures in these images could in turn make precise measuring of angles and distances difficult, as indicated above. Additionally, similar to the observations made with radiography [15], rotational positioning of the limb within the magnet leads to obliquely acquired images in the uncorrected MR pilot and could potentially result in incorrect measurements. Fitting of a ground marker that can be easily recognized, such as oil-filled capsules or a flat object with high MR signal, to the weight-bearing surface of the hoof capsule inside the radiofrequency coil could at least help to visualize essential reference points during image acquisition. This should be considered for further studies that aim to measure conformation parameters from standing low-field MR images.

In conclusion, our study has found several considerable differences between selected foot conformation parameter measurements from radiographs and from MR images that could have variable explanations. Foot conformation measurements from MR images should be used with caution in clinical practice. Limited image quality for this purpose and possible positioning artefacts associated low-field MR imaging would support the acquisition of a current set of foot radiographs at the time of MR examination.
Fig. 7

Funding

Animal welfare / Ethics approval

This is a retrospective case series.

Patient consent for publication

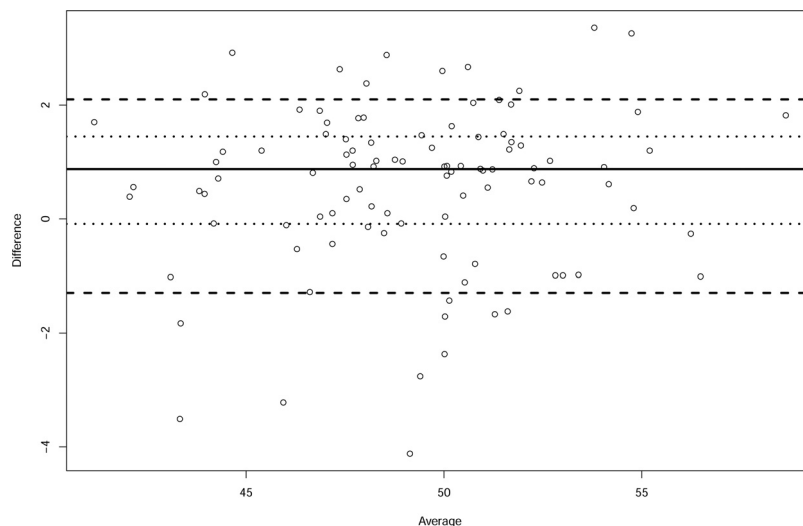Not required. Data were processed in anonymized fashion.

Fig. 7. Non-parametric Bland-Altman plot for comparison of the angles HWH Rad and HWH T1: Difference = difference between measurements in degrees, Average = mean of the measurements in degrees, top dashed line = 90th quartile, top dotted line = 75th quartile, solid line = median, bottom dotted line = 25th quartile, bottom dashed line = 10th quartile.

Table 5
Correlation matrix and Wilcoxon paired signed-rank test results of angles measured for lateromedial foot conformation.

		DistP2 M3	DistP2 M5	DistP2 Rad
DistP2 M3	Kendalls' Tau		0.60	0.43
	P value		<0.001*	<0.001*
	V		2450.50	3455.00
	P value		0.933	0.001*
DistP2 M5	Kendalls' Tau	0.60		0.39
	P value	<0.001*		<0.001*
	V	2450.50		3490.50
	P value	0.933		0.001*
DistP2 Rad	Kendalls' Tau	0.43	0.39	
	P value	<0.001*	<0.001*	
	V	3455.00	3490.50	
	P value	0.001*	0.001*	
		DistP1 M3	DistP1 M5	DistP1 Rad
DistP1 M3	Kendalls' Tau		0.59	0.40
	P value		<0.001*	<0.001*
	V		2058	2775.50
	P value		0.15	0.295
DistP1 M5	Kendalls' Tau	0.59		0.47
	P value	<0.001*		<0.001*
	V	2058		2378.00
	P value	0.15		0.615
DistP1 Rad	Kendalls' Tau	0.40	0.47	
	P value	<0.001*	<0.001*	
	V	2775.50	2378.00	
	P value	0.295	0.615	

DistP2, Angle between the distal articular surface of the middle phalanx and horizontal (coffin joint angle); DistP1, angle between the distal articular surface of the proximal phalanx and horizontal (pastern joint angle); Kendall's tau, correlation coefficient with P value; M3P, sagittal images from 3-plane MRI pilots; M5P, sagittal images from 5-plane MRI pilots; Rad, dorsopalmar radiographic view; V, V-statistic Wilcoxon paired signed-rank test with P value.
   * indicates statistical significance.

Data availability statement

All data relevant to the study are included in the article.

Declaration of Competing Interest

The authors declare no conflict of interest.

References

[1] Eliashar E. An evidence-based assessment of the biomechanical effects of the common shoeing and farriery techniques. Vet Clin North Am 2007;23:425–42.
[2] Pauwels FE, Rogers CW, Wharton H, et al. Radiographic measurements of hoof balance are significantly influenced by a horse's stance. Vet Radiol Ultrasound 2017;58:10–17.
[3] De Zani D, Polidori C, Di Giancamillo M, et al. Correlation of radiographic measurements of structures of the equine foot with lesions detected on magnetic resonance imaging. Equine Vet J 2016;48:165–71.
[4] Holroyd K, Dixon JJ, Mair T, et al. Variations of foot conformation in lame horses with different foot lesions. Vet J 2013;195:361–5.
[5] Page BT, Hagen TL. Breakover of the hoof and its effect on structures and forces within the foot. J Equine Vet Sci 2002;22:258–64.
[6] Denoix JM. Functional anatomy of the equine interphalangeal joints. Proceedings Ann Convention Am Assoc Equine Practitioners, Albuquerque NM 1999;45:174–7.
[7] Eggleston RB. Value of quality foot radiographs and their impact on practical farriery. In: Proceedings Ann Convention Am Assoc Equine Practitioners, Anaheim CA, 2012;45:164-175.
[8] Mair TS, Kinns J, Jones RD, Bolas NM. Magnetic resonance imaging of the distal limb of the standing horse. Equine Vet Educ 2005;17:74–8.
[9] Dyson SJ, Murray R. Magnetic resonance imaging evaluation of 264 horses with foot pain: The podotrochlear apparatus, deep digital flexor tendon and collateral ligaments of the distal interphalangeal joint. Equine Vet J 2007;39:340–3.
[10] Arble JB, Mattoon JS, Drost WT, et al. Magnetic resonance imaging of the initial active stage of laminitis at 4.7T. Vet Radiol Ultrasound 2009;50:3–12.
[11] Bock P, Pittermann M, Chraim M, Rois S. The inter- and intraobserver reliability for the radiological parameters of flatfoot, before and after surgery. Bone Joint J 2018;100:592–602.
[12] Tzavellas AN, Kenanidis E, Potoupnis M, et al. Interobserver and intraobserver reliability of Salter-Harris classification of physeal injuries. Hippokratia 2016;20:222–6.
[13] Grundman INM, Drost WT, Zekas LF, et al. Quantitative assessment of the equine hoof using digital radiography and magnetic resonance imaging. Equine Vet J 2014;47:542–7.
[14] Contino EK, Barrett MF, Werpy NM. Effect of limb positioning on the radiographic appearance of the distal and proximal interphalangeal joint spaces of the forelimbs of horses during evaluation of dorsopalmar radiographs. J Am Vet Med Assoc 2014;244:1186–90.
[15] Tacchio M, Davies HMS, Morgante M, Bernardini D. A radiographic technique to assess the longitudinal balance in front hooves. Equine Vet J Suppl 2002;34:368–72.
[16] Joostens Z, Evrard L, Bussoni V. Unipodal stance influences radiographic evaluation of foot balance in horses. Vet Radiol Ultrasound 2018;60:273–9.
[17] Werpy NM. Chapter 3: Low-field MRI in horses: Practicalities and image acquisition. In: Murray RC, editor. Equine MRI. Chichester, UK: Blackwell Publishing Ltd.; 2011. p. 75–99.